Proceedings of the ASME 2014 International Mechanical Engineering Congress and Exposition
IMECE2014
November 14-20, 2014, Montreal, Quebec, Canada

IMECE2014-39685

SENSITIVITY ANALYSIS OF VEHICLE PARAMETERS FOR HEADING ANGLE CONTROL OF AN UNMANNED GROUND VEHICLE

Shubhashisa Sahoo
Centre for Artificial Intelligence and Robotics
Bangalore – 560 093
Karnataka, India
sahoo6132@gmail.com

Shankar C Subramanian
Indian Institute of Technology, Madras
Chennai – 600 036
Tamilnadu, India
shankarram@iitm.ac.in

Suresh Srivastava
Office of the Director General (Aeronautics)
Bangalore – 560 093
Karnataka, India
sureshdrdo@yahoo.co.in

ABSTRACT

Even if there are many software and mathematical models available in the literature to analyze the dynamic performance of Unmanned Ground Vehicles (UGVs), it is always difficult to identify or collect the required vehicle parameters from the vehicle manufacturer for simulation. In analyzing the vehicle handling performance, a difficult and complex task is to use an appropriate tire model that can accurately characterize the ground-wheel interaction. Though, the well-known 'Magic Formula' is widely used for this purpose, it requires expensive test equipment to estimate the Magic Formula coefficients.

The design of longitudinal and lateral controllers plays a significant role in path tracking of an UGV. Though the speed of the vehicle may remain almost constant in most of the maneuvers such as lane change, Double Lane Change (DLC), step steer, cornering, etc., design of the lateral controller is always a challenging task as it depends on the vehicle parameters, road information and also on the steering actuator dynamics. Although a mathematical model is an abstraction of the actual system, the controller is designed based on this model and then deployed on the real system.

In this paper, a realistic mathematical model of the vehicle considering the steering actuator dynamics has been developed by calculating the cornering stiffnesses from the basic tire information and the vertical load on each tire. A heading angle controller of the UGV has been considered using the Point-to-Point navigation algorithm. Then, these controllers have been implemented on a test platform equipped with an Inertial Measurement Unit (IMU) and a Global Positioning System (GPS).

A wide range of experiments such as J-Turn, lane change and DLC have also been conducted for comparison with the simulation results. Sensitivity analysis has been carried out to check the robustness and stability of the controller by varying the cornering stiffness of tires, the most uncertain parameter. The longitudinal speed of the vehicle is assumed to vary between a minimum value of 1.4 m/s and a maximum value of 20 m/s. It has been found that when the vehicle is moving at a constant velocity of 3.2 m/s, a heading angle change of 20 degrees can be achieved within 3 seconds with 2% steady state error using a proportional controller. It was observed that at lower speeds, the controller is more sensitive to the steering actuator dynamics and at higher speeds, the controller is more sensitive to the cornering stiffness of tires.

INTRODUCTION

Generally, the mission plan is assigned to an UGV by using a Graphical User Interface (GUI) and its performance is monitored remotely in a control room. The navigation system of the UGV typically uses a layered architecture with different levels of abstraction to perform the assigned task. The standard architecture of the UGV comprises of three functional software levels: strategic layer, tactical layer and operational layer. The strategic layer focuses on the high-level (mission-specific) decisions. This layer determines (i) which vehicle will be used for the mission based on the size, payload and mobility systems, (ii) where the vehicle has to go from a list of routes

and (iii) the sequence and synchronization of actions such as surveillance, mine detection, mine clearance, road clearance, etc. Typically, given a goal waypoint, an Artificial Intelligence (AI) algorithm such as Dijkstra's, A*, D* (which is a dynamic version of A*) or Rapidly-exploring Randomized Trees (RRTs) helps in generating intermediate waypoints after discretizing the domain of study into a graph structure or grid structure. As the strategic layer acts as a global path planner, it must be able to estimate the approximate position of the vehicle when it approaches a node or a waypoint. Though this information does not clearly indicate how to drive or control the vehicle at this layer, these waypoints are passed down to the tactical layer for low-level planning and control of the vehicle.

Given the global path plan as a sequence of intermediate waypoints, the mobility characteristics of the vehicle (such as, skid-steering, Ackermann steering, corner steering, omni-directional, etc.,) and a representation of the environment through perception, the tactical layer plans appropriate speed and heading demands to guide the vehicle along the global path. This planning is typically carried out in a local reference frame around the vehicle. These speed and heading demands are passed on to a path tracker in the operational layer, which generates low-level motor input signals that control the steering wheel, accelerator and brake pedal. It also contains the feedback control loops to track the reference trajectories generated in the tactical layer.

Unlike in the case of holonomic motion planning, obstacles are not required to make the situation complex for a nonholonomic car-like vehicle. Continuum motion generation algorithms have not accounted for the effects of vehicle slip angle, ground-wheel interaction, steering actuator dynamics and control gain limits at the level of primitive motions. Dubins [1] showed that a sequence of three path segments which are either arcs of a circle or a straight line segment is the shortest path for a forward moving vehicle at constant speed. Much later, Reeds and Shepp [2] generalized this result to forward and backward motions and defined a set of 48 paths that contains the optimal path. Schroder et al. [3] used Dubin's method with different start and goal circles for path planning of cognitive vehicles using risk maps. These studies have been restricted to line and arc primitives based on the quest for the shortest path. In these methods, the steering angle was also assumed to change instantaneously during transition between consecutive path curvatures. Also, these geometric paths that take the UGV from the initial configuration to its goal do not comply with the dynamics of the vehicle. Therefore, if the actual motion is admissible or even possible at all, a greater control effort is required at the execution level.

Even in the absence of obstacles, there is no general algorithm to plan motions for any nonholonomic system such that the system is guaranteed to exactly reach a given goal. The only existing results are for approximate methods, which only guarantee that the system reaches a neighborhood of the goal. Obstacle avoidance adds a second level of difficulty. Particularly, an Ackermann steering or car-like vehicle has only two controls (linear and angular velocities) while it moves in a 4-dimensional configuration space (x, y, θ and ρ) where (x, y) are the coordinates of a reference point of the vehicle, θ is the orientation of the vehicle and ρ is the instantaneous curvature of the path. The admissible paths are generated by a sequence of these inputs, each of them being applied over a fixed interval of time, δt. By accounting the dynamic model of the vehicle, a significant source of error can be eliminated at the planning level rather than reactively at the execution level (in feedback control). However, many of the nonholonomic motion planning literature [4], [5] are theoretical in nature and the time required for solution generation is not often discussed.

A good vehicle simulation model plays a significant role in designing the lateral controller for an UGV. Studies on model based system identification and parameter estimation are abundant in the literature. Arikan et al. [6] reported the transfer function method approach of identifying the vehicle parameters using a dynamic bicycle model by varying the forward speed of the vehicle from 5.6 m/s to 7 m/s. Wesemeier and Isermann [7] described the method of estimating the cornering stiffness of the tire from the measurement of vehicle speed, the lateral acceleration, yaw rate and the vehicle side slip angle. Out of these, the first three measurements were available in the test vehicle, series production Opel Omega A2.0i. However, a special optical sensor was used to measure the side slip angle, β of the vehicle. The velocity of the vehicle was varied from 6 to 12 m/s to identify the model parameters using stationary driving maneuvers. Liu at al. [8] presented an iterative learning identification method of identifying a second-order model for an automated off-highway agricultural vehicle to represent the vehicle lateral dynamics.

Although there are other technical issues such as perception, communication, etc., for navigation of an UGV, only the lateral control problem related to path tracking is considered in this study. The lateral controller applies appropriate steering motions to guide the vehicle along the path as described by the vehicle path planner. To navigate an Ackermann steered vehicle at lower speeds, a realistic Point-to-Point navigation algorithm is considered for an obstacle free path. The design of the lateral controller is carried out after developing a mathematical model based on the well-known dynamic bicycle vehicle model. The challenge in designing this control system is to include the actuator dynamics, as the response time to steer the front wheel is of the same order as that of the heading angle dynamics of the vehicle. A J-turn maneuver has been carried out on a test platform to check the differences in the mathematical model and the real vehicle. Then, this model is used to estimate the look-ahead distance and the response time to achieve the desired heading angle at different velocities of the vehicle. Subsequently, the performance of the controller used in the closed loop feedback simulation was compared with the experimental results carried out on a test platform at various speeds. After that, the study has been extended to perform a DLC maneuver on the test platform. Furthermore, sensitivity analysis has been carried out by varying the speed of the vehicle and the cornering stiffness of the tires.

POINT-TO-POINT NAVIGATION

For the navigation of an Unmanned Ground Vehicle (UGV), a Point-to-Point motion algorithm is considered where the error in heading angle is used to determine the steering angle. The desired speed and heading angle of the vehicle are decided by the vehicle path planner. The state variables (X, Y, θ) can be measured from the Global Positioning System (GPS) and the Inertial Measurement Unit (IMU). In this case, (X, Y) represents the position of the vehicle and θ is the heading angle of the vehicle. If the waypoints on the path are known, the desired heading angle can be calculated from three consecutive GPS waypoints (X_0, Y_0), (X_1, Y_1) and (X_2, Y_2) are shown in Fig. 1.

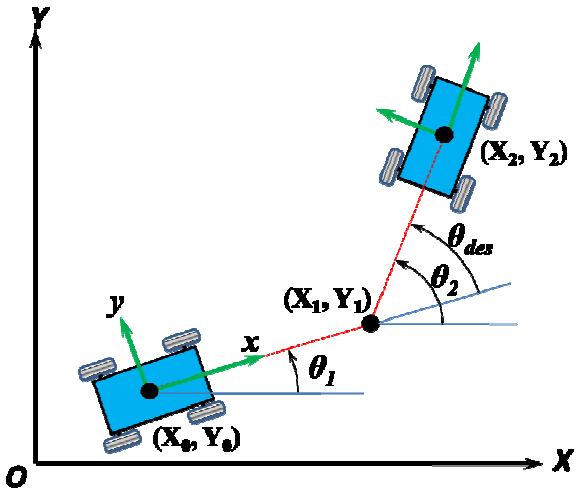

Fig. 1: Point-to-Point navigation.

The desired heading angle change, θ_{des} of the UGV is

$$\theta_{des} = \theta_2 - \theta_1. \quad (1)$$

For a waypoint to have been reached, the vehicle must pass it at a distance less than or equal to the radial tolerance for that waypoint. The mis-match between the desired heading angle and the actual vehicle heading angle under the real environment needs to be minimal to achieve good path tracking. In addition, this is significantly affected by the speed of the vehicle.

TEST PLATFORM

In this study, a commercially available 4-wheeled battery operated vehicle was modified to fulfill the experimental requirements. The front and top parts of the vehicle body were modified to accommodate the necessary electronics and sensors. The electric power was supplied from a 48V DC battery bank that could drive the vehicle with a maximum speed of 20 km/hr. The test platform after modification and mounting of equipment is shown in Fig. 2. The steering system is a self adjusting rack and pinion steering. To control the heading direction, the conventional steering system was converted to drive-by-wire by installing a DC motor (Maxon RE-40) with a 156:1 reduction gear ratio at the steering shaft. The rotation of the steering shaft can be measured by the encoder attached to the steering actuator. The steering actuator is connected to the steering shaft with the help of spur gears with a gear reduction ratio of 1.47. The standard rack and pinion steering system of the vehicle has a gear ratio of 15.5.

Fig. 2: Test platform.

The vehicle controller interprets the position of the accelerator pedal mechanism to control the wheel motor speed. This was modified to accept an input voltage generated from a higher-level controller, rather than from the accelerator pedal itself. The primary means of localization is by the use of a GPS. To cater for likely eventualities such as GPS inaccuracy, outage or denial, the system also has an accurate Inertial Navigation System (INS) onboard, which augments and is augmented by the GPS. The INS comprises a gyro-stabilized compass and the Inertial Measurement Unit (IMU).

CLOSED-LOOP FEEDBACK FOR DESIRED HEADING ANGLE

To track the desired heading angle, a closed-loop negative feedback system is considered as shown in Fig. 3.

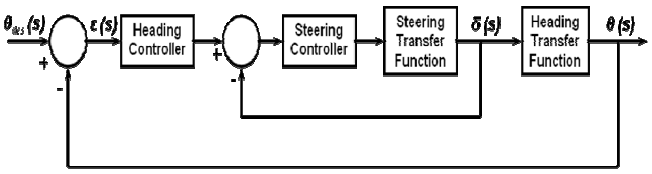

Fig. 3: Negative feedback system considering steering actuator dynamics.

The output of this model is the actual heading angle of the vehicle. The steering angle input to the vehicle depends on the desired heading angle for the given speed of the vehicle. The time taken for steering the front wheel by 10 degrees is around one second and since this is in the same order as the response time of the vehicle heading dynamics, the model of the steering actuator has been included in this study. The controller designed for this system has been decoupled into two loops. The inner loop controller, H_V^{ϕ} controls the error between the desired angular position and the current angular position of the steering motor. The input of this loop is a function of the

steering angle that is calculated based on the error in the heading angle of the vehicle. The outer loop controller, H_θ^δ decreases the error between the desired and actual heading angles of the vehicle. To perform the simulation of the system, an appropriate actuator model needs to be established. The transfer function, $G_\delta^\theta(s)$ that relates the response of the heading angle to the steering angle, is obtained by using a linearized dynamic bicycle model. The steering actuator model has been derived analytically from the electrical and mechanical governing equations that are obtained from first principles.

VEHICLE MODELING

This section describes the mathematical modeling for obtaining the heading angle transfer function of the vehicle, the tire model that is used for simulations and the modeling of the steering subsystem. To analyze the behavior of the vehicle at various driving conditions, different types of vehicle models are available in commercial vehicle simulation software packages such as ADAMS/Car, CarSim, IPG/CarMaker, etc. However, it is not easy to collect all the parameters used in the simulation from the vehicle manufacturers. Furthermore, most of these software packages use the Magic Formula [9] or other semi-empirical tire models to calculate the cornering stiffness a tire. In reality, it requires an extensive experimental facility to extract the coefficients used in these tire models. Hence, some simplifications can be considered in designing the lateral controller. Pitching and rolling motions were ignored for the planar motion of the vehicle. At low speeds, the aerodynamic influences were neglected. Further, in most of the maneuvers such as lane change, step steer, constant radius turn, etc., the speed of the vehicle remains almost constant. In addition to the aforementioned simplifications, when the weight is equally distributed on either side of the vehicle, it leads to the well-known dynamic bicycle model for an Ackerman steered vehicle.

Dynamic Bicycle Model

A simple approximation of the lateral dynamics of ground vehicles is the "bicycle model". This approximation combines the effects of the two wheels on the same axle and treats them as a single wheel positioned between the original wheels. The bicycle model of the vehicle considered in this study is shown in Fig. 4. The vehicle lateral position is measured along the lateral axis of the vehicle and the vehicle yaw angle is measured with respect to the global *X*-axis. The two degrees of freedom are represented by the vehicle lateral position, *y*, and the vehicle heading angle, θ. The lateral force at the tire-road interface depends on the slip angle. It is assumed that only the front wheel is steerable. Considering the steering angle, δ to be small, the lateral motion and yaw motion of the vehicle are governed by

$$m(\dot{v}_y + v_x r) = F_{yf} + F_{yr} \text{ and } I_z \dot{r} = l_f F_{yf} - l_r F_{yr}, \quad (2)$$

where m is the mass of the vehicle, v_x and v_y are the longitudinal and lateral velocity of the vehicle, I_z is the yaw moment of inertia of the vehicle, r is the yaw rate of the vehicle, F_{yf} and F_{yr} are lateral forces on the front and rear tires, l_f and l_r are the distances of the front and rear tires from the vehicle CG.

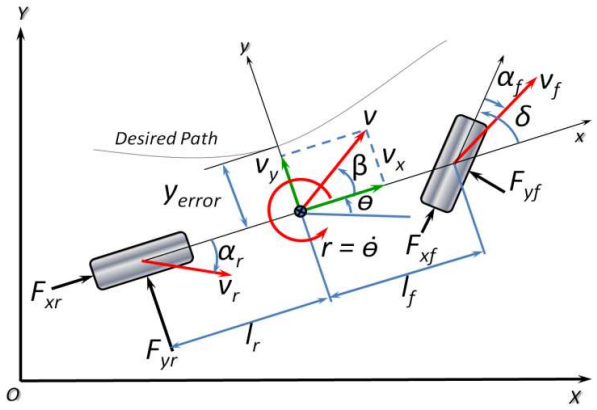

Fig. 4: Dynamic bicycle model.

Experimental results show that the lateral tire force of a tire is proportional to the slip-angle for small slip-angles [9]. The slip angle of a tire is defined as the angle between the orientation of the tire and the direction of the velocity vector at that tire. For small slip angles (α_f and α_r) of the front and rear wheels, the lateral forces acting on the front and rear wheels can be written as

$$F_{yf} = C_f \alpha_f \text{ and } F_{yr} = C_r \alpha_r, \quad (3)$$

where C_f and C_r are cornering stiffness of front and rear tires. The slip angles of the front and rear wheels are

$$\alpha_f = \delta - \left(\frac{v_y + l_f r}{v_x}\right) \text{ and } \alpha_r = -\left(\frac{v_y - l_r r}{v_x}\right). \quad (4)$$

Using equations (2), (3) and (4), the governing equation becomes

$$\begin{bmatrix} \dot{v}_y \\ \dot{r} \end{bmatrix} = \begin{bmatrix} -\frac{C_f + C_r}{m v_x} & -v_x - \frac{C_f l_f - C_r l_r}{m v_x} \\ -\frac{C_f l_f - C_r l_r}{I_z v_x} & -\frac{C_f l_f^2 + C_r l_r^2}{I_z v_x} \end{bmatrix} \begin{bmatrix} v_y \\ r \end{bmatrix} + \begin{bmatrix} \frac{C_f}{m} \\ \frac{C_f l_f}{I_z} \end{bmatrix} \delta. \quad (5)$$

The transfer function, $G_\delta^\theta(s)$ that relates the response of the heading angle to the steering angle, is obtained as

$$G_\delta^\theta(s) = \frac{a_{r1} s + a_{r2}}{s\left(s^2 + 2\xi\omega_n s + \omega_n^2\right)}, \quad (6)$$

where $a_{r1} = \frac{C_f l_f}{I_z}$, $a_{r2} = \frac{C_f C_r l}{m I_z v_x}$,

$$2\xi\omega_n = \frac{m\left(C_f l_f^2 + C_r l_r^2\right) + I_z\left(C_f + C_r\right)}{mI_z v_x} \text{ and}$$

$$\omega_n^2 = \frac{C_f C_r l^2}{mI_z v_x^2} - \frac{\left(C_f l_f - C_r l_r\right)}{I_z}.$$

The understeer coefficient, K_{us} can be written as

$$K_{us} = \frac{W_r}{C_f} - \frac{W_f}{C_r}, \quad (7)$$

where, W_f is the normal load on the front tires and W_r is that on the rear tires. The vehicle is

1 – Understeer (US), if $K_{us} > 0$

2 – Neutral steer (NS), if $K_{us} = 0$

3 – Oversteer (OS), if $K_{us} < 0$.

At the same steering wheel position and vehicle forward speed, the turning radius of an understeer vehicle is larger than that of a neutral steer vehicle and the turning radius of an oversteer vehicle is smaller than that of a neutral steer vehicle.

In a related work, Suppachai et al. [10] demonstrated the control of the heading angle of a vehicle at 1 m/s and 3 m/s. For the purpose of simulation in the absence of required vehicle parameters, the transfer function for the heading angle of the vehicle to the steering angle input was estimated empirically by manually driving the vehicle in several conditions. Hence, when it is required to implement these controllers on a different platform or at different speeds, more effort is required to estimate the transfer function coefficients. It was not discussed whether the transfer function coefficients or the vehicle parameters could be estimated at lower speeds. As the steering actuator dynamics was not considered while designing the controllers, the reference path waypoints were also found to change faster than the rate at which the steering wheel can turn.

Lee et al. [11] applied system identification techniques to obtain a system model after receiving the data from a Differential GPS (DGPS) and electric compass. To check the robustness of the developed model at different load capacities, a Sports Utility Vehicle (SUV) was initially tested at 3 m/s. Subsequently, the result was compared with an additional load of 100 kg at 5 m/s. From the simulation, they found that the tracking errors between the vehicle position and the reference path were less with the system identification method when compared with the basic bicycle model based method, but the model parameters including cornering stiffness were chosen without sufficient explanation. Also, the overshoot in yaw angles in both Proportional Integral Derivative (PID) and H_∞ controllers were more than 10 percent. In addition to that, it was not discussed how the reference path curvature was selected.

Model Parameter Estimation

From equation (6), it can be observed that, the transfer function coefficients depend on both physical and dynamic parameters of the vehicle. The dynamic mass transfer between the front and rear axles is neglected for low acceleration operations. The total mass of the vehicle, the CG location and the moment of inertia are estimated by measuring the vehicle's split mass, utilizing four measuring scales under each wheel. The total mass of the vehicle, m, is the sum of the measurements of mass under each wheel. Using these values and a measurement of the wheelbase, l, the location of CG is described by distances l_f and l_r from the front and rear axles along the center line. The moment of inertia of the vehicle is approximated by treating the vehicle as four point masses joined by a mass-less rod. The specification data for the test vehicle are listed in Tab. 1.

Parameter	Value	Unit
Mass at front-left wheel (m_{fl})	158	kg
Mass at front-right wheel (m_{fr})	137	kg
Mass at rear-left wheel (m_{rl})	360	kg
Mass at rear-right wheel (m_{rr})	269	kg
Mass of the vehicle (m)	924	kg
Wheelbase (l)	1.93	m
Location of CG from front axle (l_f)	1.31	m
Location of CG from rear axle(l_r)	0.62	m
Moment of inertia (I_z)	748	kg.m^2

Tab. 1: Parameters of the test vehicle.

However, accurate measurement of cornering stiffness of tires requires extensive experiments. In this study, to predict the vehicle behavior in a real environment and to evaluate the performance of the designed controller, simple and realistic mathematical models of the tire have been considered by calculating the cornering stiffnesses from the vertical load on each tire and also from the basic tire information. In addition to the two types of cornering stiffness data, the speed of the vehicle has been varied in the dynamic bicycle model to check the influence of these parameters in controlling the heading angle of the vehicle.

Estimating the cornering stiffness of the tire from vertical load

Pneumatic tires are important components of a wheeled vehicle. The ground-wheel interaction produces necessary forces to control the vehicle. As the cornering stiffnesses of the tires are not readily available for this vehicle, they are normalized by the vertical load. At one degree of slip angle, the average bias tire will produce a lateral force of 10 % of the vertical load. On average, radial tires have a higher cornering stiffness than bias-ply-tires. For radial tires with lower aspect ratios (0.6 and lower), it has been reported that the cornering stiffness is approximately 25%–30% of the vertical load on the tire [12]. Since the aspect ratio of the tires used in this study was 0.5, the cornering stiffness was taken as 30% of the vertical load and calculated as

$$\begin{aligned} C_{fN} &= m_f * g * 0.3\left(N/\deg\right) \\ C_{rN} &= m_r * g * 0.3\left(N/\deg\right), \end{aligned} \quad (8)$$

where g is the acceleration due to gravity, m_f is the total mass acting at the front axle, m_r is the total mass acting at the rear axle, C_{fN}, which is the cornering stiffness of the front tire, was calculated as 50000 N/rad and C_{rN}, which is the cornering stiffness of the rear tire, was calculated as 106100 N/rad.

Estimating the cornering stiffness of the tire from basic tire information

It is necessary for the tire manufacturer to print certain information such as wheel radius, tire width, aspect ratio (which is the ratio of the tire section height to tire width expressed as percentage), load index, speed rate, type of tire construction, maximum allowed inflation pressure, etc. on the tire sidewall. From this basic tire information, the cornering stiffness can be estimated by using a mathematical tire model proposed by Hewson [13]. Hewson assumed that the deflection caused by the self-aligning moment generated at the contact patch twist during cornering was prevented by the shear force to avoid any discontinuity in the tire belt. The final expression of the Hewson method that was used to estimate the cornering stiffness of the tire, C_α is

$$C_\alpha = \frac{8Ebw^3}{L\left[2\pi\left(r_w + wa\right) - L\right]} \tag{9}$$

$$\text{and } L = 2\left(r_w + wa\right)\sin\left[\cos^{-1}\left(1 - \frac{swa}{r_w + wa}\right)\right], \tag{10}$$

where E is the belt compression modulus, b is the tire belt thickness, r_w is the wheel radius, w is the belt width, a is the tire aspect ratio (tire section height/tire section width), L is the contact patch length and s is the unitized percent of sidewall vertical deflection when loaded. The parameters of the tire that are used to calculate the cornering stiffness are given in Tab. 2.

Parameter	Value	Unit
Tire aspect ratio (a)	0.5	-
Tire belt thickness (b)	0.015	m
Belt compression modulus (E)	27e6	N/m^2
Wheel radius (r_w)	0.254	m
Unitized percent of sidewall vertical deflection when loaded (s)	15 %	-
Belt width (w)	0.205	m

Tab. 2: Parameters of the tire

Of course, it is not easy to predict the tire behavior using simple measures. So, Hewson compared the predicted data with the measured data for a wide range of tires. There was a 95 percent likelihood that a predicted value was within ± 30 per cent of the actual measured value. Substituting the values of the tire parameters from Tab. 2 in eqs. (9) and (10), the tire cornering stiffness is obtained as 66300 N/rad. Since all the four tires used in the test platform are of the same specification, the cornering stiffnesses of the front and rear tires will have the same values. The estimated data for the cornering stiffness of the tires from these two methods are presented in Tab. 3. The understeer coefficient, K_{us} is calculated using eq. (7). In the absence of better data, these estimated values can be considered as a starting point for vehicle handling analysis. Hence, both the neutral steer and oversteered cases have been considered for the simulation of the dynamic bicycle model and the results are compared with the experimental data.

Estimation Method	Cornering stiffness	Value (N/rad)	Understeer coefficient
From vertical load	Front tires, C_{fN}	50000	$K_{us} = 0$ (NS)
	Rear tires, C_{rN}	106100	
Hewson method	Front tires, C_{fO}	132600	$K_{us} < 0$ (OS)
	Rear tires, C_{rO}	132600	

Tab. 3: Cornering stiffness of the tire

Modeling of the Steering Actuator

In order to maintain the vehicle heading angle, the steering wheels of the UGV should follow the command signals received from the vehicle controller and maintain synchronization with the steering actuator. The specification data for the steering actuator used are listed in Tab. 4.

Parameter	Value	Unit
Terminal resistance (R)	0.317	ohms
Terminal Inductance (L)	0.0823	mH
Torque constant (K_t)	30.2	mNm/A
Speed constant	317	rpm/V
Back emf constant (K_b)	0.0301	V/rad /sec
Rotor inertia (J)	138	g.cm^2
Speed / torque gradient	3.33	rpm / mNm
Nominal speed (N)	6930	rpm
Nominal torque (T)	170	mNm
Nominal voltage (V)	24	V

Tab. 4: Parameters of the steering actuator.

This steering actuator was used in the study of different types of controllers to control the heading angle of an UGV at a lower speed of 1.4 m/s [14]. The transfer function, $G_V^\phi(s)$ that relates the response of the angle of rotation of the steering motor shaft, $\phi(s)$, to the input voltage, $V(s)$, was derived from the first principles as [14]

$$G_V^\phi(s) = \frac{1}{s}\left(\frac{302}{0.044\ s + 9.164}\right). \tag{11}$$

SENSITIVITY ANALYSIS

The variation in the estimated cornering stiffness of tires is considered first for the sensitivity analysis. Then, the simulation is carried out for two different vehicle velocities of 3.2 and 20 m/s keeping all the other data constant. For experimental corroboration, different maneuvers such as open loop J-Turn, closed loop heading angle control and DLC have also been conducted at 3.2 m/s. The results at several test

conditions are presented to illustrate the performance of the developed controller.

J-TURN MANEUVER

A J-turn maneuver was performed on the test vehicle to corroborate the developed mathematical model. Initially, the vehicle was allowed to run for 5 seconds in a straight line to achieve a constant speed of 3.2 m/s. Then, a step steer input of 20 degrees was provided to the front wheel of the vehicle. A proportional controller was used to control the steering motor. The desired front wheel steering angle was converted to an angle of the rotation of the steering motor. The steering controller adjusts the input voltage to achieve the desired angle by calculating the corresponding error. The rotation of the motor shaft has been measured by the encoder attached to the steering motor. This angle was fed back to the steering controller. The steering angle tracking response has been simulated using eq. (11) in MATLAB-Simulink. In the simulation, the input voltage of the steering actuator was restricted from -20 to +20 Volts. However, for the smooth rotation of the steering actuator mounted in the test platform, the controller must direct the motor driver to change velocity judiciously to achieve optimum results. This is accomplished using shaped velocity profiles to limit the accelerations and decelerations required. The saturation of the steering wheel's velocity and acceleration were determined experimentally. Data were collected for the steering wheel's response to various commanded step inputs. It has been found that the proportional steering controller, H_V^{ϕ}=2, gives a better result as the maximum error is within 2 percentage when compared with the simulated result. As shown in Fig. 5, the slope of the response of the steering wheel is found to be approximately 10 degrees per second.

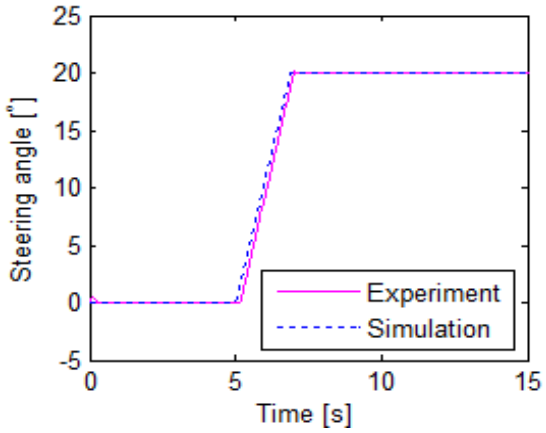

Fig. 5: Comparison of experimental and simulated steering angle input at the front wheel for J-Turn maneuver at 3.2 m/s.

For a constant vehicle speed of 3.2 m/s, the open loop response of the yaw rate to the steering angle of the vehicle can be simulated by substituting the vehicle parameters from Tab. 1 in eq. (5) for both NS and OS conditions. Similarly, eq. (6) can be used to simulate the open loop heading angle response to the steering angle input. The comparison of experimental and simulated data for vehicle yaw rate has been shown in Fig. 6. Experimental and simulated heading angle data of the vehicle are presented in Fig. 7. The cornering stiffness of tire is the only difference among the vehicle parameters that decides the NS and OS models of the vehicle. Although, C_{fO} is approximately 2.6 times of C_{fN} and C_{rO} is 1.2 times of C_{rN}, it is obvious from Fig. 6 and Fig. 7 that both NS and OS models of the vehicle closely follow the experimental results. So, for low speed navigation, a simple mathematical model will be useful in analyzing the system behavior. At the same time, it can be concluded that at a lower speed, it will be difficult to estimate the vehicle parameters uniquely. Figure 8 shows a plot of the experimentally obtained longitudinal and lateral velocities in the local coordinate.

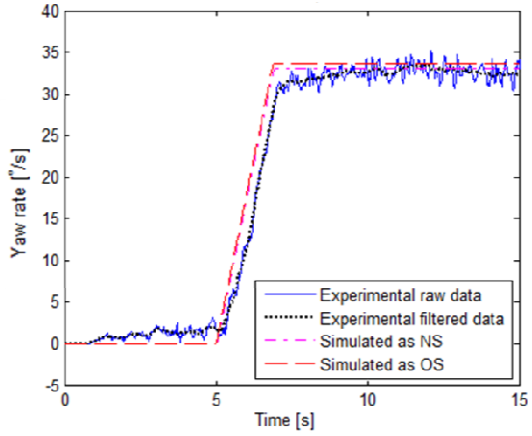

Fig. 6: Comparison of experimental and simulated yaw rate response when the vehicle is moving at 3.2 m/s.

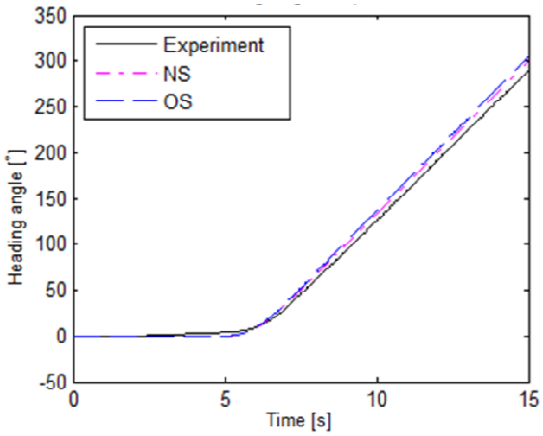

Fig. 7: Comparison of experimental and simulated heading angle response when the vehicle is moving at 3.2 m/s.

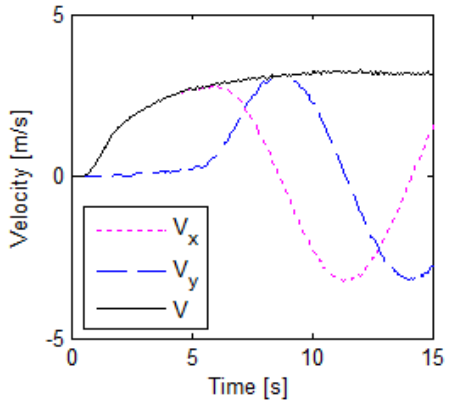

Fig. 8: Experimental velocity responses when the vehicle is moving at 3.2 m/s.

IMPLEMENTATION OF POINT-TO-POINT NAVIGATION

From eq. (7), it can be observed that the transfer function, $G_{\delta}^{\theta}(s)$, that relates the response of the heading angle to the steering angle, has a pole at the origin. So, a feedback controller as shown in Fig. 3 has to be designed to track the desired heading angle. This heading angle controller will compute the required steering angle based on the error in the heading angle of the vehicle. To analyze the effects of the steering actuator dynamics on tracking the desired heading angle at various speeds, the vehicle model was simulated at two extreme speeds of 3.2 m/s and 20 m/s. From Fig. 8, it can be observed that the UGV takes at least 7 seconds to achieve a constant speed of 3.2 m/s when started from rest. In each test performed, the vehicle was commanded to move in a straight line for 7 seconds to achieve a constant velocity and then it was commanded to achieve a desired heading angle change of 20 degrees. Experimental and simulated results for the heading angle response and the steering angle response are shown in Fig. 9 and Fig. 10 respectively.

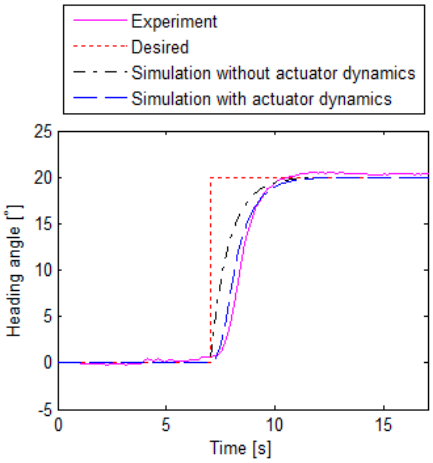

Fig. 9: Comparison of experimental and simulated results for a desired heading angle of 20 degrees with K_P = 0.7 when the vehicle is moving at 3.2 m/s.

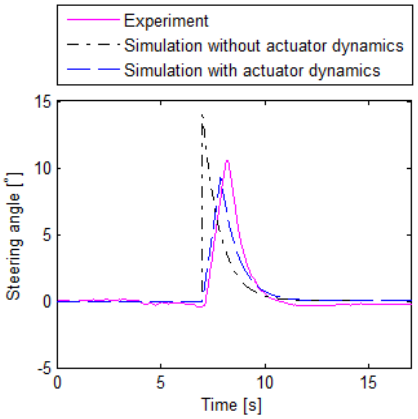

Fig. 10: Comparison of experimental and simulated results of steering angle response for desired heading angle of 20° with K_P = 0.7 when the vehicle is moving at 3.2 m/s.

A proportional controller was designed to reduce the setting time and keep the steady state error within the limit of 5 %. The maximum overshoot requirement of 10 % of steady state response results in the damping ratio, ζ, being less than 0.6. The heading angle tracking response without considering actuator dynamics has been simulated using MATLAB-Simulink and also compared while considering actuator dynamics. The proportional gain, K_P that satisfies the performance requirements was found to be 0.7 for the vehicle speed of 3.2 m/s. From the experimental data in Fig. 9, it has been found that the settling time is 2.8 seconds and the steady state error is 0.3 degrees. The steady state error is found to be less than 2% and there is no overshoot. From Fig. 10, it is observed that the maximum steering requirement has gone up to 10.5 degrees, which is well within the steering limit of the vehicle. Figure 11 shows that in comparison to the experimental data, the maximum error in the desired hearing angle is 9.1 degrees when steering actuator dynamics was not considered in the simulation. The maximum error in the heading angle has been reduced to 3.5 degrees by considering the steering actuator dynamics in the simulation.

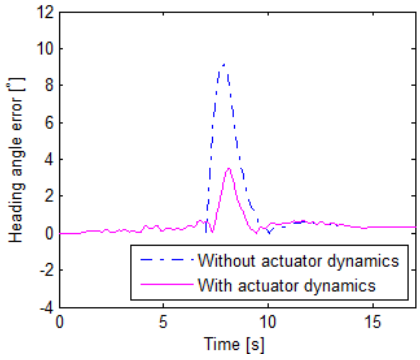

Fig. 11: Heading angle error without actuator dynamics and considering actuator dynamics when the vehicle is moving at 3.2 m/s to achieve a desired heading angle of 20 degrees.

The maximum error and the Root Mean Square (RMS) error without considering actuator dynamics are compared with the results of considering actuator dynamics in Tab. 5. It can be observed that the maximum error in steering angle has been reduced from 14.4 to 1.7 degrees by considering actuator dynamics.

Actuator dynamics	Parameter	Maximum error (deg)	RMS error (deg)
Not considered	Heading angle	9.1	2.202
	Steering angle	14.4	2.246
Considered	Heading angle	3.5	0.769
	Steering angle	1.7	0.842

Tab. 5: Error values when the vehicle is moving at 3.2 m/s.

The cornering stiffness of the tire is the most uncertain parameter for this vehicle and it decides the NS and OS models of the vehicle. However, there was no significant difference for low speed navigation of the UGV at 3.2 m/s. To analyze further, simulations were carried out for different vehicle velocities. It has been found that there was little deviation in the simulation results when the vehicle reached a speed of 10 m/s. However, there was significant difference in the performance for NS and OS models of the vehicle at 20 m/s. As, this particular experimental vehicle cannot be run at 20 m/s, only simulation results were compared for the desired heading angle in Fig. 12. The required steering angle has been shown in Fig. 13. It can be observed from Fig. 12 and Fig. 13 that when the UGV is running at a higher speed, the controller gain can be tuned in a simple manner without considering steering actuator dynamics in the simulation. However, the controller gain reduces as speed increases. As the speed of the vehicle is considered to be constant for the bicycle model, the controller needs to be tuned for different speeds and a gain scheduling method can be considered for navigation.

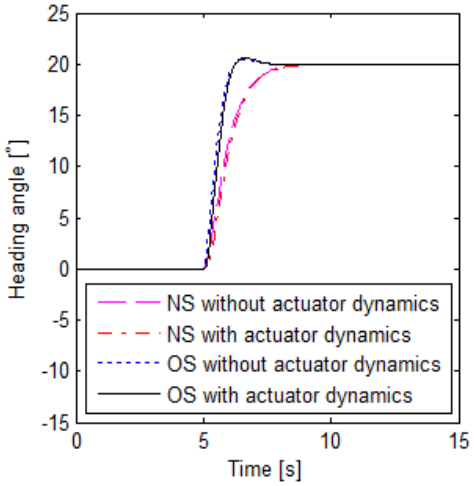

Fig. 12: Comparison of simulated results for a desired heading angle of 20^0 with proportional controller (K_P = 0.1) when the vehicle is moving at 20 m/s.

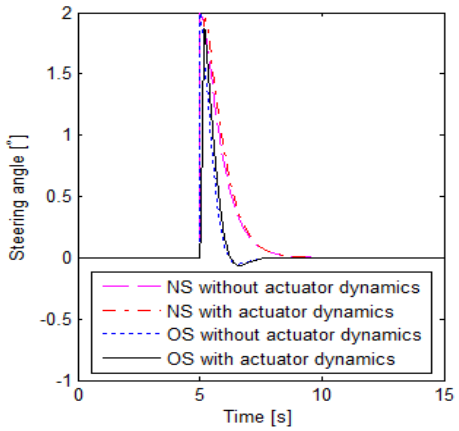

Fig. 13: Comparison of simulated results of steering angle response for desired heading angle of 20^0 with K_P = 0.1 when the vehicle is moving at 20 m/s.

DOUBLE LANE CHANGE (DLC) MANEUVER

To check the robustness of the designed controller, a double lane change maneuver was carried out for the UGV on an unpaved road. Figure 14 shows the responses of heading angle, controlled steering angles, bird's eye view of the vehicle and velocities in the longitudinal and lateral directions for the DLC maneuver.

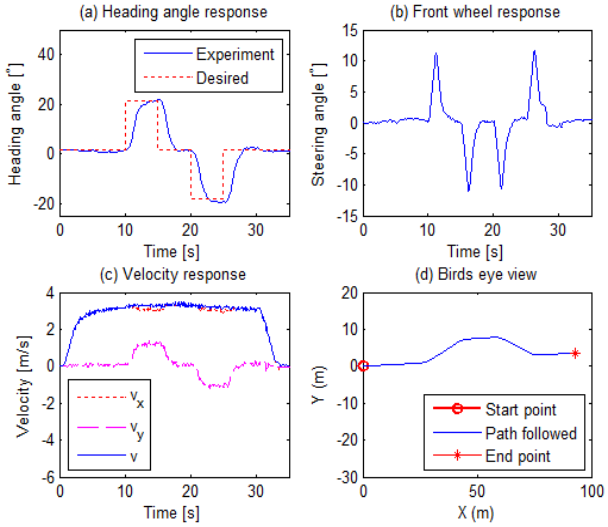

Fig. 14: Responses of heading angle, steering angle, velocities and bird's eye view of the vehicle for DLC maneuver.

Initially, the vehicle was run in a straight line for 10 seconds to achieve the speed of 3.2 m/s. Then, heading angle changes of 20 degrees were given at equal intervals of 6 seconds to complete the task. As discussed in the previous section, the UGV needs nearly 3 seconds to achieve the desired heading angle. So, when the vehicle runs at 3.2 m/s, a 3 second gap is at least required to execute the next command, else the vehicle may deviate from its planned path. A proportional controller gain, K_P = 0.7 has been used for this task.

CONCLUSION

This work has presented the analysis, design, tuning, and implementation of a heading angle controller using the dynamic bicycle model for an unmanned ground vehicle equipped with an IMU and a GPS. Moreover, the influence of vehicle parameters in controlling the heading angle of the UGV has been explained in detail. In order to achieve this, two types of tire models were used to simulate the dynamic bicycle model. The speed of the vehicle was varied from a lower speed of 3.2 m/s to 20 m/s. The following conclusions were drawn from this study:

(i) For low speed navigation of an UGV, the heading angle controller response is more sensitive to the speed of the vehicle rather than the cornering stiffness of the tires.

(ii) When the vehicle is moving at a constant velocity of 3.2 m/s, a heading angle change of 20 degrees can be achieved within 3 seconds with 2% steady state error using a proportional controller.

(iii) It is observed that the controller gain reduces as speed increases. So, the controller gain needs to be retuned for different speeds and a gain scheduling method can be considered.

(iv) Although this analysis was performed on a smaller battery operated vehicle, the proposed methodology can be easily applied to other wheeled vehicles and the controllers can be tuned faster.

(v) The look-ahead distance for the vehicle can be estimated from the response time of the heading angle controller and found to be approximately 10 m.

(vi) At higher speeds, the vehicle is less sensitive to the actuator dynamics and more sensitive to the cornering stiffness of the tires. It leads to the conclusion that the vehicle parameters may be estimated better at a higher speed.

For future work, the system model can be used to integrate lateral control and longitudinal control. From an autonomous navigation perspective, this model can be used to generate various trajectories for obstacle avoidance and path planning.

ACKNOWLEDGMENT

The authors thank the Director, CAIR for granting permission to publish the results of this research. The authors are also thankful to Mr. Nikhil Mahale at CAIR for his significant support in collecting the experimental data.

REFERENCES

[1] Dubins, L. E., 1957, “On curves of minimal length with a constraint on average curvature and with prescribed initial and terminal positions and tangents”, American Journal of Mathematics, Vol. 79, pp. 497-516.

[2] Reeds, J. A., Shepp, R. A., 1990, “Optimal paths for car that goes both forward and backward”, Pacific Journal of Mathematics, Vol. 145, No. 2, pp. 367-393.

[3] Schroder, J., Gindele, T., Jagszent, D., Dillmann, R., June 2008, “Path planning for cognitive vehicles using risk maps”, IEEE Intelligent Vehicles Symposium, pp. 1119-1125.

[4] Howard, T. M., Kelly, A., 2007, “Optimal rough terrain trajectory generation for wheeled mobile robots”, International Journal of Robotic Research, Vol. 26, No. 2, pp. 141-166.

[5] Morin, P., Samson, C., 2009, “Control of nonholonomic mobile robots based on the transverse function approach”, IEEE Transactions on Robotics, Vol. 25, No. 5, pp 1058-1073.

[6] Arıkan, K. B., Ünlüsoy, Y.S., I. Korkmaz, I., Çelebi, A. O., 2008, “Identification of linear handling models for road vehicles”, Vehicle System Dynamics, Vol. 46, No. 7, pp. 621–645.

[7] Wesemeier, D., Isermann, R., 2009, “Identification of vehicle parameters using stationary driving maneuvers”, Control Engineering Practice, Vol. 17, pp. 1426–1431.

[8] Liu, N., Alleyne, A. G., 2014, “Iterative learning identification applied to automated off-highway vehicle”, IEEE Transactions on Control Systems Technology, Vol. 22, No. 1, pp. 331-337.

[9] Bakker, E., Nyborg, L., Pacejka, H. B., 1987, “Tyre modelling for use in vehicle dynamics studies”, SAE Paper No. 870421.

[10] Suppachai, H., Silawatchananai, C., Parnichkun, M., Wuthishuwong, C., December 2009, “Double loop controller design for the vehicle’s heading control”, Proceedings of the IEEE International Conference on Robotics and Biomimetics, pp. 989-994.

[11] Lee, M. H., Lee. K. S., Park. H. G., Chun. H. H., Ryu, J. H., 2010, “Robust lateral controller for an unmanned vehicle via a system identification method”, Journal of Mechanical Systems for Transportation and Logistics, Vol. 3, No. 3, pp. 504-520.

[12] Gillespie, T. D., 1992, Fundamentals of Vehicle Dynamics, Society of Automotive Engineers, Warrendale, pp. 347-355.

[13] Hewson, P., 2005, “Method of estimating tyre cornering stiffness from basic tyre information”, Proc. IMechE Part D: Journal of Automobile Engineering, Vol. 219, pp. 1407-1412.

[14] Sahoo, S., Subramanian, S. C., Mahale, N., Srivastava, S., Accepted for publication, “Design and development of a heading angle controller for an unmanned ground vehicle”, International Journal of Automotive Technology.